Dalton Transactions

Accepted Manuscript

ROYAL SOCIETY OF CHEMISTRY

www.rsc.org/dalton

Journal Name

RSCPublishing

ARTICLE

Simple and Extremely Efficient Blue Emitters Based on Mononuclear Cu(I)-Halide Complexes with Delayed Fluorescence†

Cite this: DOI: 10.1039/x0xx00000x

Received 00th January 2012,
Accepted 00th January 2012

DOI: 10.1039/x0xx00000x

www.rsc.org/

Hiroki Ohara,[a] Atsushi Kobayashi,[a, b] and Masako Kato*[a]

Simple mononuclear Cu(I)-halide complexes, [CuX(PPh_3)$_2$(4-Mepy)] (X = Cl^-, Br^-, I^-; PPh_3 = triphenylphosphine; 4-Mepy = 4-methylpyridine), were prepared. They exhibit blue light emission with extremely high photoluminescence quantum yields approaching 100% in the crystals. The emission lifetime analyses and density functional theory calculations revealed that the bright blue light emission at room temperature are mainly delayed fluorescence originated from the singlet metal-to-ligand charge transfer (MLCT) state combined with the halide-to-ligand charge transfer (XLCT) state, (^{1}(M+X)LCT) while those at 77 K are phosphorescence from the ^{3}(M+X)LCT transition state, because of small singlet–triplet energy differences (ΔE = 940–1170 cm^{-1}). The ternary ligand systems consisting of halide, bulky phosphine, and *N*-heteroaromatic ligands provided inexpensive pure-blue-light-emitting materials by easy procedures such as simple manual grinding.

Introduction

Phosphorescent materials based on noble metal complexes, such as Ir(III) and Pt(II) complexes, have been increasingly developed for efficient light generation in organic light-emitting diodes (OLEDs).[1] Phosphorescent materials are advantageous over fluorescent materials because of their ability to harvest both singlet and triplet excitons, resulting in theoretically 100% internal quantum efficiency.[2] However, these phosphorescent materials are expensive and highly limited resources. As alternative materials, thermally activated delayed fluorescence (TADF) materials based on non-noble metal complexes and organic compounds have attracted much attention recently because they can harvest both singlet and triplet excitons.[3] When the energy difference (ΔE) between the lowest excited singlet state (S_1) and the lowest excited triplet state (T_1) is small, the singlet state can be thermally activated at the expense of the triplet state. This strategy is particularly useful for efficient electroluminescent (EL) devices.[3a,b,4] In this context, various types of TADF materials have been investigated. However, highly efficient blue-light-emitting TADF materials are still limited.[5] Zhang et al. reported efficient TADF organic compounds for blue light emission with the quantum yield, Φ = ~0.69, in toluene solution.[5a] On the other hand, Yersin and co-workers reported strong blue-luminescent Cu(I) complexes, [Cu(pop)(NN)] (pop = bis(2-(diphenyl-phosphanyl)phenyl)ether, NN = bidentate pyrazolylborate, Φ = ~0.90 in powder) and [$Cu_2(\mu$-X)$_2$(PN)$_2$] (PN = aminophosphane ligands, Φ = ~0.65 in powder), in which emissions were assigned to TADF.[5b,c] Cu(I) complexes with tetrahedral geometry have great potential for the synthesis of efficient TADF materials because of the small ΔE based on the metal-to-ligand charge transfer (MLCT) state, where the stability of the triplet state is small (<ca. 1000 cm^{-1}) owing to small exchange interactions. Thus, if a rigid structure that can suppress the deformation at the excited states is designed, Cu(I) complexes can be expected to exhibit strong luminescence based on TADF.[3b,c, 5b-d,6] In particular, Cu(I)-halide complexes bearing *N*-heteroaromatic ligands have been reported to provide systematic emitters with different emission colours from red to blue, as observed for dinuclear complexes, [$Cu_2(\mu$-X)$_2$(PPh_3)$_2$(L)$_n$] (L = *N*-heteroaromatic compounds, PPh_3 = triphenylphosphine), and [$Cu_2(\mu$-X)$_2$(P^N)$_3$] (P^N = *N*-heteroaromatic compounds with a diphenylphosphino group), by the systematic changes in the L or P^N ligands.[7] Therefore, the proper choice of *N*-heteroaromatic ligands should realise strong blue luminescent materials.

In this paper, we report simple but strongly luminescent blue light emitters based on mononuclear Cu(I)-halide complexes containing 4-methylpyridine (4-Mepy), [CuX(PPh_3)$_2$(4-Mepy)] (X = Cl^- (**1**), Br^- (**2**), and I^- (**3**); Scheme 1). We found that the blue emission of these complexes was derived from TADF with the photoluminescence quantum yields approaching 100% (for **1** and **2**) in the crystals at room temperature. Notably, the complexes **2** and **3** were also prepared by simple manual grinding.

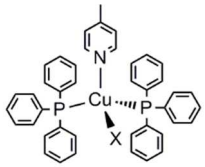

X = Cl^- (**1**), Br^- (**2**), I^- (**3**)

Scheme 1 Structure of $[CuX(PPh_3)_2(4\text{-Mepy})]$ (X = Cl^-, Br^-, I^-; 4-Mepy = 4-methylpyridine)

Experimental

Materials and synthesis

All commercially available starting materials were used as received and solvents were used without any purification. Unless otherwise stated, all manipulations were conducted in air. $[CuCl(PPh_3)_3]\cdot CH_3CN$ was prepared according to the literature procedure.[8] The ^1H NMR spectrum of each sample was measured using a JEOL EX-270 NMR spectrometer at room temperature. Elemental analysis was conducted at the analysis centre of Hokkaido University.

$[CuCl(PPh_3)_2(4\text{-Mepy})]$ (1). To $[CuCl(PPh_3)_3]\cdot CH_3CN$ (88.7 mg, 0.096 mmol) was added 4-Mepy (1 mL) and then $CHCl_3$ (1 mL). Colourless crystals were obtained by slow diffusion of diethyl ether vapour into the solution overnight. Yield: 39 mg, 56%. ^1H NMR (270 MHz, $CDCl_3$) δ ppm 2.24 (s, 3H) 7.19-7.43 (m, 34 H). Anal. Calcd for $C_{42}H_{37}NP_2ClCu$: C, 70.39; H, 5.20; N, 1.95. Found: C, 70.74; H, 5.30; N 1.91.

$[CuBr(PPh_3)_2(4\text{-Mepy})]$(2), Method 1. To a suspension of CuBr (42.5 mg, 0.30 mmol) in 4-Mepy (1 mL) was added PPh_3 (680 mg, 2.6 mmol). $CHCl_3$ (1 mL) was added to the reaction mixture and then filtered to remove precipitate. Colourless crystals were obtained by slow diffusion of diethyl ether vapour into the solution overnight. Yield: 110 mg, 47%. ^1H NMR (270 MHz, $CDCl_3$) δ ppm 2.34 (s, 3H) 7.09 (d, *J*=5.61 Hz, 2H) 7.17-7.45 (m, 30H) 8.47 (d, *J*=5.6 Hz, 2H), Anal. Calcd for $C_{42}H_{37}NP_2BrCu$: C, 66.27; H, 4.90; N, 1.84. Found: C, 66.17; H, 4.92; N 1.84. **Method 2.** CuBr (39.4 mg, 0.27 mmol), PPh_3 (136 mg, 0.52 mmol) and 4-Mepy (0.24 mL, 2.5 mmol) were added to an agate mortar. The materials were ground with a pestle for a few minutes. The resulting white solid was added to Et_2O to remove unreacted ligands and impurity, and then collected by filtration, washed with Et_2O, and dried in air. ^1H NMR spectrum of the white solid was consistent with the crystalline sample obtained by Method 1 and the PXRD pattern was consistent with the simulated pattern based on the single crystal of **2** (Fig. S1). Yield: 102 mg, 49%.

$[CuI(PPh_3)_2(4\text{-Mepy})]$ (3), Method 1. To a suspension of CuI (48.9 mg, 0.26 mmol) in 4-Mepy (1 mL) was added PPh_3 (660 mg, 2.5 mmol) and then $CHCl_3$ (1 mL). Colourless crystals were obtained by slow diffusion of diethyl ether vapour into the solution for 1week. Yield: 177.1 mg, 85%. ^1H NMR (270 MHz, $CDCl_3$) δ ppm 2.34 (s, 3H) 7.08 (d, *J*=5.6 Hz, 2H) 7.17-7.47 (m, 30H) 8.43-8.50 (m, 2H). Anal. Calcd for $C_{42}H_{37}NP_2ICu$: C, 62.42; H, 4.61; N, 1.73. Found: C, 62.50; H, 4.63; N 1.75.

Method 2. CuI (49 mg, 0.26 mmol), PPh_3 (130 mg, 0.50 mmol) and 4-Mepy (0.24 mL, 2.5 mmol) were added to an agate mortar. The materials were ground with a pestle for a few minutes. The resulting white solid was added to Et_2O to remove unreacted ligands and impurity, and then collected by filtration, washed with Et_2O, and dried in air. ^1H NMR spectrum of the white solid was consistent with the crystalline sample obtained by Method 1 and the PXRD pattern was consistent with the simulated pattern based on the single crystal of **3** (Fig. S1). Yield: 177 mg, 85%.

Luminescence measurements

The luminescence spectrum of each sample was measured using a JASCO FR-6600 spectrofluorometer at room temperature. The slit widths of the excitation and emission light were 5 and 6 nm, respectively. The luminescence quantum yield was recorded on a Hamamatsu Photonics C9920-02 absolute photoluminescence quantum yield measurement system equipped with an integrating sphere apparatus and 150-W CW Xenon light source. Hamamatsu Photonics A10095-03 non-luminescent quartz sample holder was used for absolute photoluminescence quantum yield measurements of the solid samples in air atmosphere. The accuracy of the instrument was confirmed by the measurement of the quantum yield of anthracene in ethanol solution (Φ = 0.27).[9] Emission life time measurements were conducted by using a Hamamatsu Photonics, C4334 system equipped with a streak camera as a photo detector and a nitrogen laser for the 337 nm excitation. A liquid N_2 cryostat (Optistat-DN optical Dewar and ITC-503 temperature controller, Oxford Instruments) was used for the temperature control.

Single crystal X-ray diffraction measurements

All single crystal X-ray diffraction measurements were conducted using a Rigaku Mercury CCD diffractometer with graphite monochromated Mo Kα radiation (λ = 0.71069 Å) and a rotating anode generator. Each single-crystal was mounted on a MicroMount using paraffin oil. The crystal was then cooled using an N_2-flow type temperature controller. Diffraction data were collected and processed using the CrystalClear softwere.[10] Structures were solved by the direct method using SIR-2004[11] for **1**, SIR-97[12] for **2** and SIR-2002[13] for **3**. Structural refinements were conducted by the full-matrix least-squares method using SHELXL-97.[14] Non-hydrogen atoms were refined anisotropically, and hydrogen atoms were refined using the riding model. All calculations were conducted using the Crystal Structure crystallographic software package.[15] Crystallographic data obtained for each complex are summarized in Table 1 and deposited to Cambridge Crystallographic Data Centre (CCDC 986415–986417).

Powder X-ray diffraction measurements

Powder X-ray diffraction was conducted using a Bruker D8 Advance diffractometer equipped with a graphite monochro-

Table 1 Crystal parameters and refinement data.

	1	2	3
T / K	200 (1)	200 (1)	200 (1)
Formula	$C_{42}H_{37}ClCuNP_2$	$C_{42}H_{37}BrCuNP_2$	$C_{42}H_{37}ICuNP_2$
Formula weight	716.71	761.16	808.16
Crystal system	Monoclinic	Triclinic	Triclinic
Space group	$P2_1/n$	P–1	P–1
a / Å	9.973(3)	11.4725(6)	11.641(3)
b / Å	24.648(6)	16.0533(11)	16.112(5)
c / Å	15.235(4)	19.838(2)	19.967(6)
α / °	90	100.594(5)	100.657(5)
β / °	101.227(3)	93.054(4)	92.322(5)
γ / °	90	94.306(2)	94.296(3)
V / Å^3	3673(2)	3572.9(5)	3664(2)
Z	4	4	4
D_{cal} / g cm^{-3}	1.296	1.415	1.465
Reflections collected	28176	27989	53612
Unique reflections	8328	15717	16658
R_{int}	0.0500	0.0272	0.0511
GOF	1.091	1.070	1.134
$R_1{}^a$ ($I > 2\sigma(I)$)	0.0456	0.0403	0.0556
$wR_2{}^b$ (all data)	0.1193	0.1042	0.1400

$^a R_1 = \Sigma||F_o| - |F_c||/\Sigma|F_o|$. $^b wR_2 = [\Sigma w(F_o^2 - F_c^2)/\Sigma w(F_o)^2]^{1/2}$, $w = [\sigma_c^2(F_o^2) + (xP)^2 + yP]^{-1}$, $P = (F_o^2 - 2F_c^2)/3$.

meter using Cu-Kα radiation and one-dimensional LinxEye detector.

Theoretical Calculations

DFT calculations were performed with B3LYP functional[16] and the LANL2DZ basis[17] set using Gaussian 03 program.[18] Molecular structures determined by X-ray crystallographic analysis were used. Molecular orbitals were shown using Avogadro 1.10.[19]

Results and discussion

Syntheses of mononuclear Cu(I) complexes

The mononuclear Cu(I) complex **1**, was synthesized simply by mixing $[CuCl(PPh_3)_3]$ and 4-Mepy in $CHCl_3$. Interestingly, complexes **2** and **3** were prepared from simple materials such as CuX (X = Br^-, I^-), PPh_3, and 4-Mepy without using any solvent as in the case of relevant mononuclear Cu(I) complexes $[CuI(PPh_3)_2L]$ (L = isoquinoline, 1,6-naphthyridine, pyridine) which we reported very recently.[20] After mixing CuX and PPh_3 with the ratio of 1:2 in a drop of 4-Mepy (around 10 equimolar amounts), products were obtained that emitted blue luminescence under UV light (Method 2). The colourless block crystals of complexes **1**–**3** were produced by the slow diffusion of diethyl ether to $CHCl_3$ solutions including $[CuCl(PPh_3)_3]$ and 4-Mepy or CuX (X = Br^-, I^-), PPh_3 and 4-Mepy.

Crystal structures

X-ray crystallography revealed that complexes **1**–**3** adopt a mononuclear tetrahedral coordination geometry occupied by one halide, one N atom of 4-Mepy, and two P atoms of PPh_3 (Fig. 1(a–e)). Only one crystallographically independent Cu(I) complex molecule was observed in complex **1**, whereas two independent molecules (**A** and **B**) were observed in complexes **2** and **3**. This is probably due to the steric effects of larger halides (Br^- and I^-) in complexes **2** and **3**. The torsion angle between the 4-Mepy ring and Cu–X bond of complex **1** (ca. 29°) is smaller than those of complexes **2** and **3** (47–53°). The two P atoms of complex **1** are coordinated symmetrically with respect to the Cu–X bond, while those of complexes **2** and **3** are coordinated asymmetrically showing the relatively larger distortion (Table 2). These structural differences indicate that large halide ions such as Br^- and I^- caused steric repulsion between the two PPh_3 ligands, and this steric repulsion create a space which gave rise to the conformational flexibility of the 4-Mepy ligand for complexes **2** and **3**.

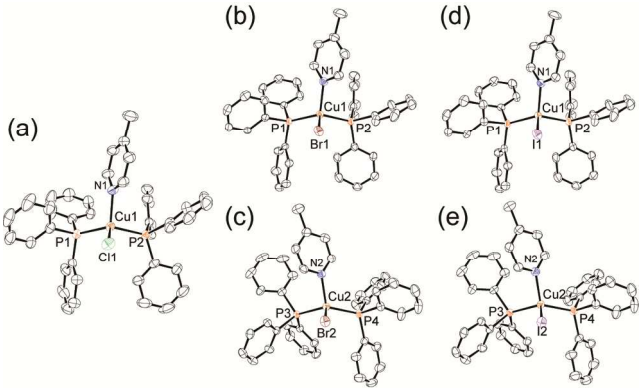

Fig. 1. ORTEP drawings of (a) complex **1**, (b) and (c) two independent molecules of complex **2A** and **B**, and (d) and (e) two independent molecules of complex **3A** and **B**, respectively. Hydrogen atoms are omitted for clarity. Displacement parameters are drawn at 50% probability level.

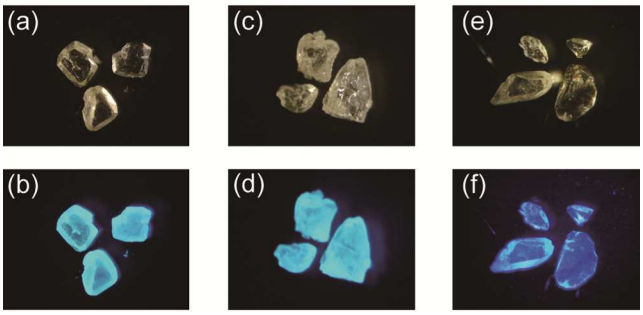

Fig. 2. Photographs of crystals **1**(a and b), **2**(c and d) and **3**(e and f) under bright field and UV light, respectively.

Luminescence properties

Crystals of **1**–**3** exhibit strong blue luminescence when they are excited with UV light as shown in Fig. 2. In solution, however, these complexes are unstable to give rise to partially ligand dissociation, dimerization and oxidation as in the case of many other Cu(I)-halide complexes.[5c,7a] Thus, the luminescence measurements were performed with crystalline samples. Fig. 3 shows the emission spectra at room temperature and 77 K. All the complexes, **1**–**3**, provide similar broad emission spectra without vibronic progression, indicating that the emissive

Table 2 Selected bond lengths, torsion angles and bond angles of **1–3**.

	1	2		3	
		A	B	A	B
Cu1(Cu2)–X [a] / Å	2.3092(9)	2.4762(5)	2.4604(4)	2.6594(10)	2.6443(9)
Cu1(Cu2)–N1(N2) / Å	2.103(2)	2.119(2)	2.113(3)	2.119(4)	2.116(5)
Cu1(Cu2)–P1(P3) / Å	2.2539(8)	2.2671(8)	2.2880(7)	2.2745(14)	2.301(1)
Cu1(Cu) –P2(P4) / Å	2.2725(7)	2.2923(7)	2.2659(7)	2.2915(15)	2.279(2)
X–Cu1(Cu2)–N1(N2)–C (4Mepy) [a] / °	29.0(1)	47.4(1)	-53.3(1)	46.7(3)	-53.0(3)
P1(P3)–Cu1(Cu2)–X [a] / °	106.04(3)	105.77(2)	111.61(2)	104.35(4)	110.63(4)
P2(P4)–Cu1(Cu2)–X [a] / °	107.11(3)	111.28(2)	104.29(3)	111.99(4)	103.99(4)

[a] X = Cl1, Br1, Br2, I1 and I2 for **1**, **2A**, **2B**, **3A**, and **3B**, respectively

Table 3 Luminescence properties of complexes **1–3** in the solid states at 298 K and 77 K.

Complex	1		2		3	
	298 K	77 K	298 K	77 K	298 K	77 K
λ_{max} [a] (nm)	468	488	467	477	455	458
τ (μs (A_n))[b]	5.8 (0.43)	18.3 (0.17)	9.6 (0.38)	41.0 (0.59)	3.9 (0.67)	46.1 (0.67)
	10.7 (0.64)	38.0 (0.82)	16.6 (0.72)	61.9 (0.47)	11.5 (0.52)	61.5 (0.36)
Φ [c]	0.99	0.82	0.95	0.95	0.66	0.76
τ_{av} [d] (μs)	9.4	36	15	52	9.5	52
k_r [e] (s^{-1})	1.1×10^5	2.3×10^4	6.3×10^4	1.8×10^4	6.9×10^4	1.4×10^4
k_{nr} [f] (s^{-1})	1.1×10^3	5.0×10^3	3.3×10^3	9.5×10^2	3.6×10^4	4.4×10^3

[a] Emission maximum. [b] Emission lifetime. [c] Emission decays were analysed with two components: $I = A_1\exp(-t/\tau_1) + A_2\exp(-t/\tau_2)$. [c] Photoluminescence quantum yields in the solid states. [d] Average emission lifetimes were determined by using eq. 1. [e] Radiative rate constants k_r were estimated by Φ/τ_{av}. [f] Nonradiative rate constants k_{nr} were estimated by $k_r(1 - \Phi)/\Phi$.

excited states have a charge-transfer property. Each emission spectrum at 77 K shifted to lower energies by ca. 940–1230 cm^{-1} than that at room temperature. Regarding the effect of halide ligands, the emission spectra of iodide complex **3** appeared at shorter wavelength regions compared to those of complexes **1** and **2**, even though the difference is very small. A similar trend was observed for more commonly used halide-bridged dinuclear complexes.[3c,5c,7c] Along with the emission maxima, photoluminescence quantum yields and lifetimes at room temperature and at 77 K are listed in Table 3. Notably, these simple complexes exhibit very high quantum yields at room temperature (0.99 for complex **1**, 0.95 for complex **2**, and 0.66 for complex **3**, respectively). The emission lifetimes of **1–3** in the crystals were estimated by the least-square fitting of the emission decays using two exponentials, i.e., $I = A_1\exp(-t/\tau_1) + A_2\exp(-t/\tau_2)$, where τ_1 and τ_2 are the lifetimes and A_1 and A_2 are the pre-exponential factors. Because the time-resolved emission spectra in the crystals are unchanged during the entire decay, the two decay components are considered to be the emission from different sites with the same electronic origin (Fig. S2). The lifetimes of complexes **1–3**, with the values ranging from several microseconds to several tens of microseconds at room temperature, are similar to those previously reported for Cu(I) complexes such as $[Cu_2(\mu\text{-}X)_2(PPh_3)_2(L)_n]$[7a] and [CuX(dtpb)][21] (dtpb = 1,2-bis(*o*-ditolylphosphino)benzene), whose luminescence was assigned to phosphorescence, and $[Cu_2(\mu\text{-}I)_2(dppb)_2]$ and [CuI(dppb)PPh_3] (dppb = 1,2-bis[diphenylphosphino]benzene), which showed delayed fluorescence at room temperature.[3c] Thus, the blue luminescence of complexes **1–3** may have a similar origin. Then, the radiative rate constants (k_r) of complexes **1–3** were estimated from the average emission lifetime (τ_{av}) by using equation (1)[22] for two exponential decay components:

$$\tau_{av} = \frac{A_1\tau_1^2 + A_2\tau_2^2}{A_1\tau_1 + A_2\tau_2} \qquad (1)$$

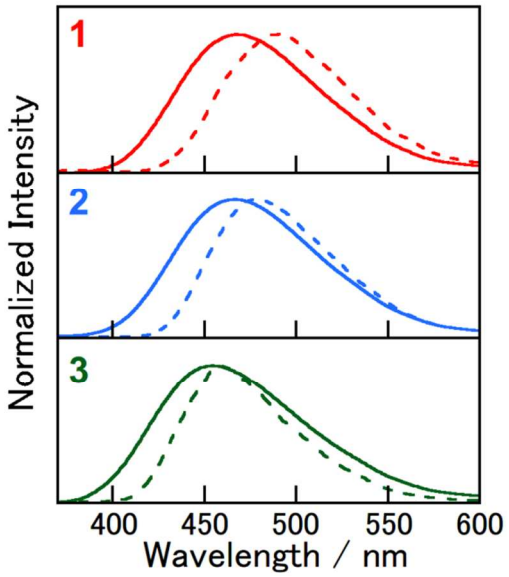

Fig. 3 Luminescence spectra of complexes **1–3** in the solid states (λ_{ex} = 350 nm) at room temperature (solid lines) and 77 K (dotted lines).

The τ_{av} of complexes **1–3** and k_r, which was estimated by using the relation $k_r = \Phi/\tau_{av}$, and the nonradiative rate constants k_{nr} are also listed in Table 3. The results indicate that the radiative constants at 298 K are in a similar range (k_r = 6–11 × 10^4 s^{-1}),

while a difference was observed in the nonradiative rate constants. Iodide complex **3** has a much larger value (k_{nr} = 3.6 × 10^4 s^{-1}) than the others (k_{nr} = 1–3 × 10^3 s^{-1} for complexes **1** and **2**), suggesting that the flexible orientation of 4-Mepy in the crystal could increase in the nonradiative deactivation for **3** at room temperature, in particular. For all the complexes, the radiative constants at room temperature are several times larger than those at 77 K, indicating that the origins of the emissions at 298 and 77 K are different.

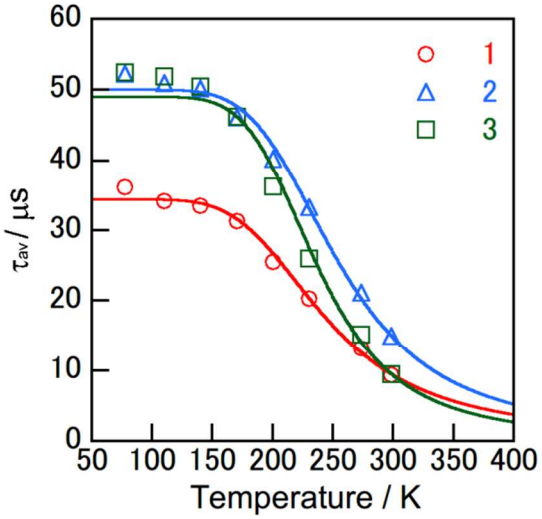

Fig. 4 Temperature dependence of the average emission lifetimes of complexes **1**–**3** in the solid states. The solid lines were calculated by using eq. 2.

Table 4 Fitting parameters based on the two-state model (eq. 2).

	1	**2**	**3**
ΔE [a]	940 cm^{-1}	1070 cm^{-1}	1170 cm^{-1}
$\tau(S_1)$ [b]	47 ns	41 ns	14 ns
$\tau(T_1)$ [b]	34 μs	50 μs	49 μs

[a] Energy difference between S_1 and T_1. [b] lifetimes of the S_1 and T_1 states determined by the fitting using eq. 2 using the averaged emission lifetimes.

Emission lifetime analyses

To describe the two emission states quantitatively, temperature dependence of the average emission lifetimes of complexes **1**–**3** was investigated (Fig. 4). From 77 K to 170 K, the lifetimes changed gradually for all the complexes. However, at higher temperatures above 170 K, a sharp decrease in the lifetimes was observed. Assuming the two-state model involving the lowest excited singlet state (S_1) and the lowest excited triplet state (T_1), the observed lifetime can be expressed as a Boltzmann average by using equation (2).[4b, 5c, d, 6, 23]

$$\tau_{obs} = \frac{3+exp(-\Delta E/RT)}{3/\tau_{T_1}+1/\tau_{S_1}exp(-\Delta E/RT)} \quad (2)$$

where, ΔE is the energy difference between the singlet and triplet states, τ_{S1} and τ_{T1} are the lifetimes of S_1 (fluorescence) and T_1 (phosphorescence) states, R is the ideal gas constant, and T is the absolute temperature. In this two-state model analysis, average lifetime was used instead of τ_{obs}, i.e., τ_{obs} = τ_{av}. The corresponding fitting parameters are listed in Table 4. The obtained ΔE values (940, 1070, and 1170 cm^{-1} for complexes **1**, **2** and **3**, respectively) are roughly consistent to the spectral shifts of ~1000 cm^{-1} between 298 and 77 K, indicating that the two-state model is reasonable in the temperature region. The values are also comparable to those reported for several Cu(I) complexes.[3b,c, 4b, 5b-d, 6, 24] At room temperature, the emissions of complexes **1**–**3** occur mainly from the singlet state by efficient up-conversion. Using fitting parameters, singlet components of luminescence ($I(S_1)/I_{total}$) can be estimated by using equation (3) [5c]

$$\frac{I(S_1)}{I_{total}} = 1 - \left(1 + \frac{\Phi_{S1}\tau_{T1}}{3\Phi_{T1}\tau_{S1}}exp(-\Delta E/RT)\right)^{-1} \quad (3)$$

where, Φ_{S1} and Φ_{T1} are luminescence quantum yields of the singlet and triplet states. Assuming the values of Φ_{S1} and Φ_{T1} to those of Φ at 298K and 77K, respectively, the singlet components at 298 K can be roughly estimated to be 76%, 70% and 78% for complexes **1**, **2** and **3**, respectively. The energy difference between the singlet and triplet states increases in the order of complexes **1**, **2** and **3**. This is probably related to the lowering of the emission quantum efficiency of complex **3** because a larger population in the triplet state with smaller rate constants (i.e., longer lifetime) should be affected by the nonradiative decay. Thus, iodide complex **3** with the largest ΔE has the lowest quantum efficiency (0.66 at 298 K) among the three complexes. On the other hand, almost 100% quantum yield is achieved by chloride complex **1** with the smallest ΔE (940 cm^{-1}), even though the value is not so small compared to those reported (e.g., 460-630 cm^{-1} for $[Cu_2(\mu\text{-}X)_2(PN)_2]$).[5c] This proves the superior properties of these simple mononuclear complexes.

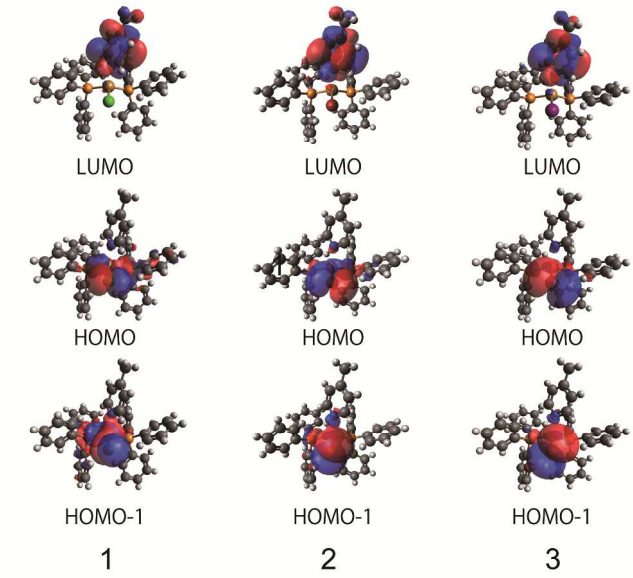

Fig. 5 Molecular orbitals of complexes **1**–**3**.

Theoretical calculations

To determine the emissive excited states of complexes **1**–**3**, time dependent-density functional theory (TD-DFT) calculations were carried out for complexes **1**–**3** using the atomic coordinates determined by X-ray crystallographic analysis (Fig. 5 and see ESI). The electron density in the highest occupied molecular orbital (HOMO) and HOMO-1 are distributed over the Cu and halogen atom, while that in the lowest unoccupied molecular orbital (LUMO) is localized on the 4-Mepy ligand. For complexes **2** and **3**, the HOMO–LUMO transition contributes to the lowest excited state by 100%. For complex **1**, the HOMO–LUMO and HOMO-1–LUMO transitions contribute to the lowest excited state by 26 and 74%, respectively. Thus, the lowest excited states of complexes **1**–**3** are assignable to the combined MLCT and halide-to-ligand charge transfer (XLCT) states, ((M+X)LCT).

Possible mechanism of luminescence

Scheme 2 shows the schematic luminescent mechanism diagram of complexes **1**–**3**. At room temperature, the ^{1}(M+X)LCT state is thermally accessible from the ^{3}(M+X)LCT emissive state because of the small ΔE (940–1170 cm^{-1}). Thus, all the complexes, **1**–**3**, mainly emit delayed fluorescence from the ^{1}(M+X)LCT state at room temperature. On the other hand, at low temperatures below 170 K, complexes **1**–**3** emit phosphorescence from the ^{3}(M+X)LCT state because the ^{1}(M+X)LCT state cannot be thermally activated at the expense of the ^{3}(M+X)LCT state. Thermal activation efficiency could affect the luminescence quantum yields at 298K. For the chloride complex **1**, which has the lowest ΔE value (940 cm^{-1}) among the three, the decrease in the luminescence quantum yield from 0.99 at 298K to 0.82 at 77K can be explained by the suppression of TADF at low temperature. For the iodide complex **3**, however, the luminescence quantum yield at 298K (0.66) is lower than those of the others due to the larger nonradiative deactivation process as discussed in the previous section (see Table 3). As a result, relatively higher quantum yield would be obtained at 77 K because of effective suppression of nonradiative decay process (i.e. smaller k_{nr}) at low temperature compared to that at room temperature. The complex **2** with the intermediate value of ΔE and the relatively small k_{nr} even at room temperature is considered to have the very high quantum yield (0.95) both at 298 K and 77 K.

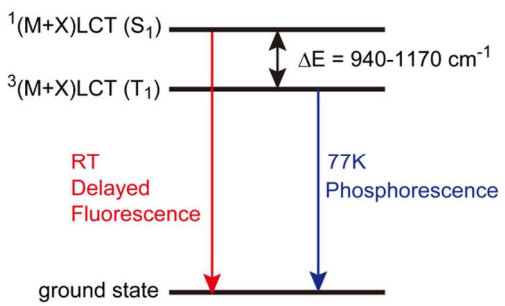

Scheme 2 Schematic diagram of the two-state model of complexes **1**–**3**.

Conclusions

In conclusion, we prepared three mononuclear Cu(I)-halide complexes containing 4-Mepy ligand, complexes **1**–**3**, that show strong blue luminescence in the crystals, exhibiting almost 100% quantum yields for complexes **1** and **2**. The emission studies and TD-DFT calculations reveal that complexes **1**–**3** emit TADF from the ^{1}(M+X)LCT state at room temperature because of their small singlet–triplet energy difference. In addition, these complexes can be easily prepared from commercially available inexpensive reagents such as CuX, 4-Mepy, and PPh_3. Such an efficient synthesis of desired strong emitters from simple starting materials without difficult procedures should be one of the important factors for their applications. In our recent work, we demonstrated that the emission colour of the mononuclear Cu(I)-iodide complexes [CuI(PPh_3)$_2$(L)] are varied by changing L;[20] thus, efficient red-to-blue light-emitting TADF Cu(I) complexes can be obtained by the proper choice of L ligands. The relevant mononuclear Cu(I) complexes containing various L ligands are under investigation.

Acknowledgements

This work was partially supported by Grants-in-Aid for Scientific Research (B) (23350025), Artificial Photosynthesis (No. 2406), Young Scientists (B) (24750049) from the Ministry of Education, Culture, Sports, Science and Technology (MEXT), Japan.

Notes and references

[a] *Department of Chemistry, Faculty of Science, Hokkaido University, North-10 West-8, Kita-ku, Sapporo, Hokkaido 060-0810, Japan.*
Fax: +81-11-706-3447; Tel: +81-11-706-3817;
E-mail: mkato@sci.hokudai.ac.jp
[b] *A Precursory Research for Embryonic Science and Technology (PRESTO), Japan Science and Technology Agency (JST), Honcho 4-1-8, Kawaguchi, Saitama 332-0012, Japan.*

† Electronic Supplementary Information (ESI) available: PXRD patterns of **2** and **3**, emission decays, time-resolved emission spectra, details of DFT calculations, and ^{1}H NMR spectra of **1**–**3**. See DOI: 10.1039/b000000x/

1 (*a*) L. Xiao, Z. Chen, B. Qu, J. Luo, S. Kong, Q. Gong and J. Kido, *Adv. Mater.*, 2011**,** **23**, 926; (*b*) Y. Chi and P. -T. Chou, *Chem. Soc. Rev.*, 2010, **39**, 638.

2 (*a*) C. Adachi, M. A. Baldo, M. E. Thompson and S. R. Forrest, *J. Appl. Phys.*, 2001, **90**, 5048; (*b*) H. Sasabe, J. Takamatsu, T. Motoyama, S. Watanabe, G. Wagenblast, N. Langer, O. Molt, E. Fuchs, C. Lennartz and J. Kido, *Adv. Mater.*, 2010, **22**, 5003; (*c*) M. A. Baldo, D. F. O'Brien, Y. You, A. Shoustikov, S. Sibley, M. E. Thompson and S. R. Forrest, *Nature*, 1998, **395**, 151; (*d*) M. A. Baldo, S. Lamansky, P. E. Burrows, M. E. Thompson and S. R. Forrest *Appl. Phys. Lett.*, 1999**,** **75**, 4; (*e*) Y. Kawamura, K. Goushi, J. Brooks, J. J. Brown, H. Sasabe and C. Adachi, *Appl. Phys. Lett.*, 2005, **86**, 071104.

3 (*a*) H. Uoyama, K. Goushi, K. Shizu, H. Nomura and C. Adachi, *Nature*, 2012, **492**, 234; (*b*) J. C. Deaton, S. C. Switalski, D. Y. Kondakov, R. H. Young, T. D. Pawlik, D. J. Giesen, S. B. Harkins, A. J. M. Miller, S. F. Mickenberg and J. C. Peters, *J. Am. Chem. Soc.*,

2010, **132**, 9499; (*c*) A. Tsuboyama, K. Kuge, M. Furugori, S. Okada, M. Hoshino and K. Ueno, *Inorg. Chem.*, 2007, **46**, 1992.

4 (*a*) S. Igawa, M. Hashimoto, I. Kawata, M. Yashima, M. Hoshino and M. Osawa, *J. Mater. Chem. C*, 2013, **1**, 542; (*b*) Q. Zhang, T. Komino, S. Huang, S. Matsunami, K. Goushi and C. Adachi, *Adv. Funct. Mater.*, 2012, **22**, 2327.

5 (*a*) Q. Zhang, J. Li, K. Shizu, S. Huang, S. Hirata, H. Miyazaki and C. Adachi, *J. Am. Chem. Soc.*, 2012, **134**, 14706; (*b*) R. Czerwieniec, J. Yu and H. Yersin, *Inorg. Chem.*, 2011, **50**, 8293; (*c*) M. J. Leitl, F. R. Kuchle, H. A. Mayer, L. Wesemann and H. Yersin, *J. Phys. Chem. A*, 2013, **117**, 11823; (*d*) X. -L. Chen, R. Yu, Q. -K. Zhang, L. -J. Zhou, X. -Y. Wu, Q. Zhang and C. -Z. Lu, *Chem. Mater.*, 2013, **25**, 3910.

6 R. Czerwieniec, K. Kowalski and H. Yersin, *Dalton Trans.*, 2013, **42**, 9826.

7 (*a*) H. Araki, K. Tsuge, Y. Sasaki, S. Ishizaka and N. Kitamura, *Inorg. Chem.*, 2005, **44**, 9667; (*b*) D. M. Zink, D. Volz, T. Baumann, M. Mydlak, H. Flügge, J. Friedrichs, M. Nieger and S. Bräse, *Chem. Mater.*, 2013, **25**, 4471; (*c*) D. M. Zink, M. Bächle, T. Baumann, M. Nieger, M. Kuhn, C. Wang, W. Klopper, U. Monkowius, T. Hofbeck, H. Yersin and S. Bräse, *Inorg. Chem.*, 2013, **52**, 2292.

8 T. Kräuter and B. Neumüller, *Polyhedron*, 1996, **15**, 2851.

9 (*a*) W. R. Dawson and M. W. Windsor, *J. Phys. Chem.*, 1968, **72**, 325; (*b*) W. H. Melhuish, *J. Phys. Chem.*, 1961, **65**, 229.

10 *CrystalClear*, Molecular Structure Corporation, Orem, UT, 2001.

11 *SIR-2004*: M. C. Burla, R. Caliandro, M. Camalli, B. Carrozzini, G. L. Cascarano, L. De Caro, C. Giacovazzo, G. Polidori and R. Spagna, *J. Appl. Crystallogr.*, 2005, **38**, 381.

12 *SIR-97*: A. Altomare, M. C. Burla, M. Camalli, G. L. Cascarano, C. Giacovazzo, A. Guagliardi, A. G. Moliterni, G. Polidori and R. Spagna, *J. Appl. Crystallogr.*, 1999, **32**, 115.

13 *SIR-2002*: M. C. Burla, M. Camalli, B. Carrozzini, G. L. Cascarano, C. Giacovazzo, G. Polidori and R. Spagna, *J. Appl. Crystallogr.*, 2003, **36**, 1103.

14 *SHELX97*: G. M. Sheldrick, *Acta Crystallogr., Sect. A:Fundam. Crystallogr.,* 2008, **64**, 112.

15 *CrystalStructure 4.0*: Rigaku Corporation, Tokyo, Japan, 2000-2010.

16 (*a*) A. D. Becke, *J. Chem. Phys.*, 1993, **98**, 5648; (*b*) C. Lee, W. Yang and R. G. Parr, *Physical Review B*, 1988, **37**, 785.

17 (*a*) P. J. Hay and W. R. Wadt, *J. Chem. Phys.*, 1985, **82**, 270; (*b*) W. R. Wadt and P. J. Hay, *J. Chem. Phys.*, 1985, **82**, 284; (*c*) P. J. Hay and W. R. Wadt, *J. Chem. Phys.*, 1985, **82**, 299.

18 M. J. Frisch, G. W. Trucks, H. B. Schlegel, G. E. Scuseria, M. A. Robb, J. R. Cheeseman, J. A. Montgomery, Jr., T. Vreven, K. N. Kudin, J. C. Burant, J. M. Millam, S. S. Iyengar, J. Tomasi, V. Barone, B. Mennucci, M. Cossi, G. Scalmani, N. Rega, G. A. Petersson, H. Nakatsuji, M. Hada, M. Ehara, K. Toyota, R. Fukuda, J. Hasegawa, M. Ishida, T. Nakajima, Y. Honda, O. Kitao, H. Nakai, M. Klene, X. Li, J. E. Knox, H. P. Hratchian, J. B. Cross, C. Adamo, J. Jaramillo, R. Gomperts, R. E. Stratmann, O. Yazyev, A. J. Austin, R. Cammi, C. Pomelli, J. W. Ochterski, P. Y. Ayala, K. Morokuma, G. A. Voth, P. Salvador, J. J. Dannenberg, V. G. Zakrzewski, S. Dapprich, A. D. Daniels, M. C. Strain, O. Farkas, D. K. Malick, A. D. Rabuck, K. Raghavachari, J. B. Foresman, J. V. Ortiz, Q. Cui, A. G. Baboul, S. Clifford, J. Cioslowski, B. B. Stefanov, G. Liu, A. Liashenko, P. Piskorz, I. Komaromi, R. L. Martin, D. J. Fox, T. Keith, M. A. Al-Laham, C. Y. Peng, A. Nanayakkara, M. Challacombe, P. M. W. Gill, B. Johnson, W. Chen, M. W. Wong, C. Gonzalez and J. A. Pople, *Gaussian 03 (Revision E.01)*, Gaussian, Inc., Wallingford CT, 2004.

19 M. D. Hanwell, D. E. Curtis, D. C. Lonie, T. Vandermeersch, E. Zurek and G. R. Hutchison, *J. Cheminform.,* 2012, **4**, 17.

20 H. Ohara, A. Kobayashi and M. Kato, *Chem. Lett.*, 2014, **43**, 1324.

21 M. Hashimoto, S. Igawa, M. Yamashita, I. Kawata, M. Hoshino and M. Osawa, *J. Am. Chem. Soc.*, 2011, **133**, 10348.

22 J. R. Lakowicz, *Principles of Fluorescence Spectroscopy*, Springer, New York, 2006, pp. 141-142.

23 J. R. Kirchhoff, R. E. Gamache Jr, M. W. Blaskie, A. A. Del Paggio, R. K. Lengel and D. R. McMillin, *Inorg. Chem.*, 1983, **22**, 2380.

24 M. S. Asano, K. Tomiduka, K. Sekizawa, K. Yamashita and K. Sugiura, *Chem. Lett.*, 2010, **39**, 376.

Graphical abstract

Title: Simple and Extremely Efficient Blue Emitters Based on Mononuclear Cu(I)-Halide Complexes with Delayed Fluorescence

Authors: Hiroki Ohara, Atsushi Kobayashi and Masako Kato

Mononuclear Cu(I)-halide complexes with a ternary ligand system exhibit blue light emission based on delayed fluorescence with extremely high quantum yields, approaching 100% in the solid states.